

THE PATHOGENESIS OF VIRAL INFLUENZAL PNEUMONIA IN MICE

M. J. PLUMMER, M.S.,* AND R. S. STONE, M.D.†

*From the Department of Pathology, University of California
School of Medicine, Los Angeles, Calif.*

Recognizable descriptions of the clinical aspects of influenza are found in writings from the 16th century onward, although the disease no doubt existed prior to this time. During the pandemic of 1889, it was believed that the disease resulted from the inhalation of a "ground poison" or a noxious miasma. However, a bacterial etiology was favored by most authorities when the great influenza pandemic of 1918-1919 occurred. Since that time, interest in all aspects of the disease has grown, and its viral etiology has been established.¹

Early physicochemical studies of the influenza virus indicated a unit size of 100 m μ and resistance of viral infectivity to trypsin digestion.²⁻⁴ The biologic properties of the virus were studied by producing experimental infections, first in ferrets, then in mice and other laboratory animals.⁵⁻⁹ Descriptions of human influenza were made from necropsy material by Hers¹⁰ and others.¹¹⁻¹³

Many morphologic studies of the virus by electron microscopy were performed using intact viruses¹⁴⁻¹⁸ and sectioned tissue.¹⁹⁻²¹ The infectious virus was found to be a spherical unit, 100 m μ in diameter, and composed of two subunits—the S or soluble antigen, and the V or viral antigen which were released upon treatment with ether.²² Hers, Mulder, Masurel, Kuip and Tyrell²³ studied the pathogenesis of influenzal pneumonia using fluorescent antibody staining techniques with antibodies specific for these antigens.

Although many light microscopic studies of the pathogenesis of influenza have been performed, there are still unanswered problems, and little work has been done by electron microscopy. The present study was undertaken in order to investigate the pathogenesis of influenzal pneumonia in mice by electron microscopy. Efforts were made to correlate these findings with those obtained by simultaneous light microscopy.

Partially supported by United States Public Health Service grant C5565-03.

Accepted for publication, February 18, 1964.

* Submitted in partial fulfillment of the requirements for the degree of Master of Science, University of California, Los Angeles, Calif.

† Present address: Department of Pathology, School of Medicine, University of New Mexico, Albuquerque, N.M.

MATERIAL AND METHODS

A pool of virus stock was made up from infected mouse lung, using influenza virus A, strain PR8, as the infecting virus. The stock was divided into 1 ml. samples, frozen in a dry-ice alcohol bath and stored at -70° C. until used. This virus stock was used in all the experiments described in this paper. Efforts were made to inoculate each animal used in the experimental procedures with an equal amount of virus, so that the resultant infections would be comparable. Table I shows a titration of the virus stock in which an infecting dose of 1.5 LD₅₀ was used. This small infecting dose was chosen in order to minimize the nonspecific toxic effects produced by large inoculums of virus.

TABLE I
TITRATION OF STOCK INFLUENZA VIRUS *

Time (days)	EID ₅₀ †	HT ‡	C §
1	10 ^{-9.2}	1:640	0, 0, 0
2	10 ^{-8.5}	1:2560	±, ±, 0
3	10 ^{-8.2}	1:160	2+, 0, 0
4	10 ^{-8.0}	1:1280	3+, 2+, ±
5	10 ^{-7.9}	1:320	2+, +, +
6	10 ^{-7.0}	1:10	2+, ±, ±
7	10 ^{-6.5}	0	3+, 3+, ±

* The mice used in this titration were inoculated with 1.5 LD₅₀ of stock PR8 influenza virus. The lungs from 3 mice were pooled for each determination.

† EID₅₀, 50 per cent embryo infectivity end point.

‡ HT, hemagglutinin titer.

§ C, amount of lung consolidation determined by gross examination and scored on a 0 to 4 point basis. The score for each of the 3 mice is recorded.

Under light ether anesthesia, 4-week-old Swiss mice were inoculated intranasally with 1.5 LD₅₀ of the mouse-adapted strain of PR8 influenza virus stock. At daily intervals up to 1 week, 3 to 5 mice were anesthetized by the intraperitoneal administration of 10 per cent urethane, and the thoracic organs were exposed. The lungs were perfused with approximately 5 cc. of 1 per cent buffered phosphate osmium tetroxide by injecting the fixative into the right cardiac ventricle. The lungs then were quickly removed, minced into small fragments, and retained in iced osmium tetroxide for 45 minutes. After washing in phosphate buffer, the tissue fragments were dehydrated in graded alcohols, passed through propylene oxide, and embedded in Epon resin. Sectioning was performed with glass knives using both the Porter-Blum and LKB microtomes. The sections for light microscopy, approximately 1.5 μ in thickness, were stained with toluidine blue prior to examination. Sections for electron microscopy were stained with uranyl acetate, uranyl acetate and lead monoxide, or uranyl acetate and phosphotungstic acid. Examination was performed with an Hitachi HU 11-A electron microscope at 50 kv. Most sections were mounted on copper grids without the aid of a supporting film.

RESULTS

The Normal Mouse Lung

The ultrastructure of the normal mouse lung has been extensively investigated by many workers; ²⁴ the present work essentially confirms

the earlier findings. Initial studies²⁵ raised some question as to the existence of a continuous epithelial lining covering the alveolar surface, and it was thought that the pulmonary capillaries came into direct contact with the alveolar air. However, it was finally demonstrated²⁶ and established²⁴ that a continuous alveolar epithelial lining does exist. The following description of the ultrastructure of the normal mouse lung is based upon our observations; these are in agreement with those of previous investigators.

The alveolar epithelial cytoplasm was stretched over a very wide surface area, thus making the nucleus of the cell appear to bulge into the alveolar lumen. The cytoplasmic organelles were concentrated in the perinuclear zone, and the peripheral sheets of attenuated cytoplasm contained few structural components other than a few pinocytotic vesicles. Supporting the epithelium was a basement membrane, usually homogeneous in appearance, although it might contain a few fibrillar structures. Also adjacent to the basement membrane were the capillary endothelial cells which appeared indistinguishable from the alveolar lining epithelial elements. In the peripheral lung parenchyma, there was a complete lack of interstitial tissue, and the blood-air pathway consisted merely of a thin layer of epithelial cytoplasm, a basement membrane, and a thin layer of endothelial cytoplasm (Figs. 1 and 2). Scattered macrophages, located adjacent to the alveolar lining cells were occasionally seen in the normal alveolus. They were large, irregular cells in close contact with the alveolar wall and often contained dense, osmiophilic bodies in their cytoplasm, probably representing phagocytized debris.

Bronchioles were located in close proximity to the vascular channels and consisted of several well-defined structural layers. Larger bronchioles were lined by stratified epithelium, including ciliated, non-ciliated, and goblet cells. The smaller air passages, however, possessed only a single row of ciliated and nonciliated cells (Fig. 1). No goblet cells were present. The nonciliated cells were columnar with rounded luminal surfaces and contained many dense mitochondria. The endoplasmic reticulum was very well developed and consisted of numerous tiny vesicles and tubular structures. The ciliated cells were cuboidal, sometimes appearing to be overshadowed by the neighboring non-ciliated cells, and many cilia projected from their luminal surface. There were fewer mitochondria and a less well-developed endoplasmic reticulum than was seen in the nonciliated cells. Supporting the epithelium was a basement membrane and a thin layer of elastica. Smooth muscle, in variable amounts, was observed peripheral to the elastica,

while loose collagenous connective tissue with a few fibroblasts and macrophages comprised the outer portion of the bronchiolar wall. The smallest bronchioles communicated with the alveolar air spaces where gaseous exchange took place.

Infected Mouse Lung

The infected animals became ill 24 to 48 hours after viral inoculation. Movements were limited, and respiration became progressively more rapid and labored until death ensued. A few animals did not die and recovered from the infection.

Because the early lesions were patchy in distribution and varied from animal to animal, it was necessary to examine the lungs by light microscopy to select appropriate lesions for electron microscopic study. Correlation of observations was necessary, therefore, for the complete interpretation of pulmonary lesions.

Lesions in infected animals were seen earlier by electron than by light microscopy and were usually present within 24 hours of inoculation. These occurred in the alveolar septums and thickened the blood-air pathway from 3 to 4 times its normal thickness. The attenuated layer of epithelial cytoplasm lining the alveolar air spaces showed focal areas of intracellular edema, occasionally with the formation of large intracytoplasmic vesicles. The cellular organelles, as in the normal state, remained concentrated in the perinuclear region, and little structure other than a few vesicles and amorphous granular material was apparent in the edematous foci (Figs. 3 and 4). The cell limiting membrane was distorted by this intracellular accumulation of fluid and occasionally ruptured, with subsequent barring of the underlying basement membrane. The cell membrane, even in nonedematous areas became irregular in outline and often formed microvilli. Similar lesions were observed in the capillary endothelium, although not to the same degree (Fig. 5). The nuclei of both these cell types hypertrophied and the cells were enlarged. Edematous foci were noted within the basement membrane, which separated the epithelium from the endothelium (Fig. 6). Granular debris, perhaps representing portions of damaged cells, was sometimes observed within the swollen regions of the basement membrane.

The first change visible by light microscopy was observed 2 to 3 days after viral inoculation. At this time, the alveolar septums appeared thickened because of hyperemia and apparent cellular infiltration of the alveolar walls. The higher magnification of the electron microscope permitted clarification of the nature of this change.

Capillary dilatation and congestion and the intracellular lesions previously described contributed to the thickening of the septums. How-

ever, macrophage proliferation was the primary cause of the septal hypercellularity and thickening seen by light microscopy. The macrophages, infrequently seen in sections of normal lung, were situated in the lumens of alveoli in close proximity to the alveolar lining cells; by light microscopy they appeared to be actually within the alveolar wall. The dense, osmiophilic bodies in the macrophage cytoplasm, usually interpreted as representing phagocytized debris, were often increased in number. The cell outlines were irregular, and pseudopod-like cytoplasmic projections were frequent.

The first indication of cellular response in the bronchioles was noted 3 days after infection in the nonciliated epithelial lining (Figs. 7 and 8). The endoplasmic reticulum of these cells became hypertrophied and assumed various abnormal arrangements. Although parallel rows of flattened cisternae or tubules are occasionally observed in normal bronchiolar cells, many such laminated arrangements were present in the infected lungs. Small groups of mitochondria were surrounded by circumferential laminae of flattened cisternae and vesicles. Often the small vesicles appeared to be arising from thin, tubular components of the endoplasmic reticulum (Fig. 8). Cytoplasmic edema, especially in the apical portions of these cells, was commonly observed. The ciliated cells in the bronchioles were not affected in this manner and appeared unchanged at this time.

Proliferation of influenza virus was seen only at the lumen surface of the nonciliated bronchiolar epithelium (Figs. 9 and 10). The virus differentiated from small, finger-like projections of cytoplasm, which then pinched off to form a free, mature viral particle. Most viral particles were spherical in shape and consisted of a dense nucleoid surrounded by a peripheral layer of radially oriented rods. As is typical of the myxoviruses, pleomorphic forms were often seen, although filamentous "incomplete" virus was not observed. The cytoplasm of the virus-producing cells was edematous and contained many thin, filamentous strands which perhaps represented viral ribonucleoprotein (Fig. 10).

As the disease progressed, many of the bronchiolar lining cells showed degenerative changes. Osmiophilic, granular bodies of varying sizes were often present in both ciliated and nonciliated cells, sometimes almost filling the cell, compressing and displacing the nucleus (Fig. 11). Focal and generalized intracellular edema gave a thin, watery appearance to the cytoplasm, and irregularly-shaped lipid droplets became a conspicuous feature of the degenerating cells. The latter sloughed from the wall, and the bronchiolar lumens eventually became filled with desquamated necrotic cells and cellular debris. The regenerating bronchiolar epithelium underwent a metaplastic change and assumed

a stratified appearance, with the surface cells becoming elongated and flattened. These cells, too, showed evidence of degeneration and necrosis, and often sloughed from the wall. The peribronchiolar connective tissue, which normally contains very few cells, became completely infiltrated with cells, mostly of the mononuclear type (Fig. 12).

The lesions in the peripheral portions of the lung progressed in a similar manner. The macrophages, which previously had been in close contact with the alveolar lining cells, rounded up and detached from the alveolar wall, showing degenerative changes. The epithelial lining underwent necrosis and sloughed from the wall into the air spaces (Fig. 13). Many of these cells, however, remained close to their original location and enhanced the light-microscopic appearance of alveolar septal thickening with cellular infiltration. Eventually, the alveolar air spaces became completely consolidated by the desquamated cells (Fig. 14). There was no evidence of capillary thrombosis, but the endothelium showed foci of edema and necrosis, although actual sloughing did not occur.

DISCUSSION

Although the inoculation of each mouse with an equal amount of virus was attempted, there was considerable variation in the severity of the lesions produced at any specific time interval. The small differences in inoculating doses, as well as individual animal variation, undoubtedly were contributing factors. However, there was a steady progression from the first ultramicroscopic lesions seen at about 24 hours, through phases of cellular proliferation and necrosis, to the massive alveolar consolidation and peribronchiolar inflammation 1 week after viral inoculation.

Specific measures to prevent secondary bacterial infection were not employed, but there was no evidence to suggest that such contamination had taken place, and the pneumonia produced seemed to be the result of the viral infection alone.

Studies by Hers and co-workers,²³ using fluorescent antibody staining techniques, revealed the presence of V and S viral antigens in both bronchial and alveolar lining cells shortly after the intranasal inoculation of influenza virus. This suggested that the virus entered the alveolar lining cells and that the initial lesions seen in these cells were the result of the viral infection, although cellular reaction to local concentrations of foreign material in the alveoli could not be excluded. Production of viral particles at the surface of these cells was not observed in the present study.

The alveolar lining cells contain few mitochondria, and the endoplasmic reticulum is sparse, which implies a low rate of oxidative phos-

phorylation and protein synthesis. In addition, the organelles are concentrated in the perinuclear region and possibly support nuclear metabolism. It may be, therefore, that although the virus infects these cells and causes cellular degeneration, the metabolic rate of the cells is inadequate to support viral growth and development, especially in the peripheral cytoplasmic areas where the early lesions occur. Examination of the cells which did support viral proliferation, that is, the nonciliated bronchiolar epithelial cells, revealed many dense mitochondria and an abundance of endoplasmic reticulum throughout the cytoplasm. The endoplasmic reticulum consistently appeared hyperplastic prior to the release of mature viral particles at the cell membrane. It seems reasonable to suppose that the hyperplastic endoplasmic reticulum was synthesizing viral protein, supported by energy produced by the numerous mitochondria. The filamentous strands noted in the cytoplasm of the virus-producing cells possibly represented viral ribonucleoprotein, incorporated into mature virus at the cell surface.

The granular, osmiophilic bodies described by Harford, Hamlin and Parker²⁷ as microcolonies of viral particles were also observed in the present study (Fig. 11). However, these inclusions were not confined to the virus-producing cells but were frequently observed in the bronchiolar ciliated cells as well. There was no evidence to relate them directly to viral maturation or proliferation. Mature viral particles were never seen within cells, and it is believed that these bodies represented a nonspecific inclusion commonly found in degenerating cells.

The inflammation of viral pneumonia has long been described as interstitial in character. The infiltration of mononuclear cells into the peribronchiolar and perivascular spaces undoubtedly could be classified in this manner. However, the peripheral lesions consisted of intra-alveolar consolidation from lining cell macrophage proliferation, not a cellular infiltrate into the alveolar septums, and thus cannot be called interstitial in nature. Because of the relatively low magnification of the light microscope, it is difficult to differentiate alveolar septal cell types and to identify the original alveolar wall after the alveolar lining cells have hypertrophied and sloughed. It is understandable, therefore, that the septal thickening due to cell hypertrophy, edema and macrophage proliferation has been interpreted as cellular infiltration into the septums. It is only with the higher magnification of the electron microscope that the lesions may be satisfactorily differentiated.

SUMMARY

The pathogenesis of influenzal pneumonia in mice was studied by electron microscopy. Mice were inoculated with 1.5 LD₅₀ of PR8 influenza virus and killed at varying intervals after inoculation. Observa-

tions by light microscopy were correlated with those by electron microscopy in order to evaluate the lesions produced.

At the periphery, the earliest lesions were focal areas of edema of alveolar lining cells, the capillary endothelium and the interposed basement membrane. This caused an appreciable thickening of the blood-air pathway. Hypertrophy, degeneration and desquamation of the alveolar lining and proliferation of alveolar macrophages resulted in complete consolidation, which was progressive up to 1 week after infection.

The central areas of the lung were affected somewhat differently. At 3 days after infection, the nonciliated bronchiolar cells showed considerable hyperplasia of endoplasmic reticulum and apical cytoplasmic edema. Viral particles matured at the lumen surface of these cells and were then released into the bronchiolar lumen. The bronchiolar cells, both ciliated and nonciliated, underwent degeneration and sloughed into the bronchiolar lumen. The regenerating epithelium was stratified, and the surface cells were elongated and flattened. The peribronchiolar interstitial tissue gradually became totally infiltrated by cells, mostly of the mononuclear type.

REFERENCES

1. SMITH, W.; ANDREWES, C. H., and LAIDLAW, P. P. A virus obtained from influenza patients. *Lancet*, 1933, 2, 66-68.
2. LENNETTE, E. H., and HORSFALL, F. L., JR. Studies on epidemic influenza virus; nature and properties of the complement-fixing antigen. *J. Exper. Med.*, 1940, 72, 233-246.
3. ELFORD, W. J.; ANDREWES, C. H., and TANG, F. F. The sizes of the viruses of human and swine influenza as determined by ultrafiltration. *Brit. J. Exper. Path.*, 1936, 17, 51-53.
4. MERRILL, M. H. Effect of purified enzymes on viruses and gram-negative bacteria. *J. Exper. Med.*, 1936, 64, 19-28.
5. STRAUB, M. The microscopical changes in the lungs of mice infected with influenza virus. *J. Path. & Bact.*, 1937, 45, 75-78.
6. GINSBERG, H. S., and HORSFALL, F. L., JR. Quantitative aspects of the multiplication of influenza A virus in the mouse lung; relation between the degree of viral multiplication and the extent of pneumonia. *J. Exper. Med.*, 1952, 95, 135-145.
7. TAYLOR, R. M. Experimental infections with influenza A virus in mice; increase in intrapulmonary virus after inoculation and influence of various factors thereon. *J. Exper. Med.*, 1941, 73, 43-55.
8. STUART-HARRIS, C. H. Influenza and Other Virus Infections of the Respiratory Tract. Edward Arnold & Co., Ltd., London, 1953, 235 pp.
9. LOOSLI, C. G. The pathogenesis and pathology of experimental air-borne influenza virus A infections in mice. *J. Infect. Dis.*, 1949, 84, 153-168.
10. HERS, J. F. PH. The Histopathology of the Respiratory Tract in Human Influenza. H. E. Stenfort Kroese, N. V., Leiden, 1955.

11. SCADDING, J. G. Lung changes in influenza. *Quart. J. Med.*, 1937, 6, 425-465.
12. STRAUB, M., and MULDER, J. Epithelial lesions in the respiratory tract in human influenzal pneumonia. *J. Path. & Bact.*, 1948, 60, 429-434.
13. MULDER, J., and VERDONK, G. J. Studies on the pathogenesis of a case of influenza-A pneumonia of three day's duration. *J. Path. & Bact.*, 1949, 61, 55-61.
14. MOSLEY, V. M., and WYCKOFF, R. W. G. Electron micrography of the virus of influenza, *Nature, London*, 1946, 157, 263.
15. MURPHY, J. S.; KARZON, D. T., and BANG, F. B. Studies of influenza A (PR 8) infected tissue cultures by electron microscopy. *Proc. Soc. Exper. Biol. & Med.*, 1950, 73, 596-599.
16. HOLLÓS, I. Electronmicroscopic examination of complete and incomplete influenza virus particles. *Acta microbiol., hung.*, 1957, 4, 459-474.
17. HOLLÓS, I. Electronmicroscopic examination of complete and incomplete influenza virus. III. Examination of the fine structure of complete influenza virus by disintegration and digestion methods. *Acta microbiol., hung.*, 1960, 7, 57-64.
18. HOYLE, L.; HORNE, R. W., and WATERSON, A. P. The structure and composition of the myxoviruses. II. Components released from the influenza virus particle by ether. *Virology*, 1961, 13, 448-459.
19. EDDY, B. E., and WYCKOFF, R. W. G. Influenza virus in sectioned tissues. *Proc. Soc. Exper. Biol. & Med.*, 1950, 75, 290-293.
20. MORGAN, C.; ROSE, H. M., and MOORE, D. H. Structure and development of viruses observed in the electron microscope. III. Influenza virus. *J. Exper. Med.*, 1956, 104, 171-182.
21. HOLLÓS, I., and BARNA, A. Electronmicroscopic examination of complete and incomplete influenza viruses. II. Studies of the fine structure of complete influenza viruses. *Acta microbiol., hung.*, 1958, 5, 387-397.
22. DAVENPORT, F. M.; ROTT, R., and SCHAEFER, W. Physical and biological properties of influenza virus components obtained after ether treatment. *J. Exper. Med.*, 1960, 112, 765-782.
23. HERS, J. F.; MULDER, J.; MASUREL, N.; KUIP, v.d.L., and TYRELL, D. A. Studies of the pathogenesis of influenza virus pneumonia in mice. *J. Path. & Bact.*, 1962, 83, 207-217.
24. SCHULZ, H. Die submikroskopische Anatomie und Pathologie der Lunge. Springer-Verlag, Berlin, 1959.
25. MACKLIN, C. C. Pulmonic alveolar epithelium; report of round table conference. *J. Thoracic Surg.*, 1936, 6, 82-88.
26. LOW, F. N. The pulmonary alveolar epithelium of laboratory mammals and man. *Anat. Rec.*, 1953, 117, 241-263.
27. HARFORD, C. G.; HAMLIN, A., and PARKER, E. Electron microscopy of early cytoplasmic changes due to influenza virus. *J. Exper. Med.*, 1955, 101, 577-590.

We wish to acknowledge the invaluable help of Dr. Margret I. Sellers, Department of Medical Microbiology and Immunology, University of California, Los Angeles.

[Illustrations follow]

LEGENDS FOR FIGURES

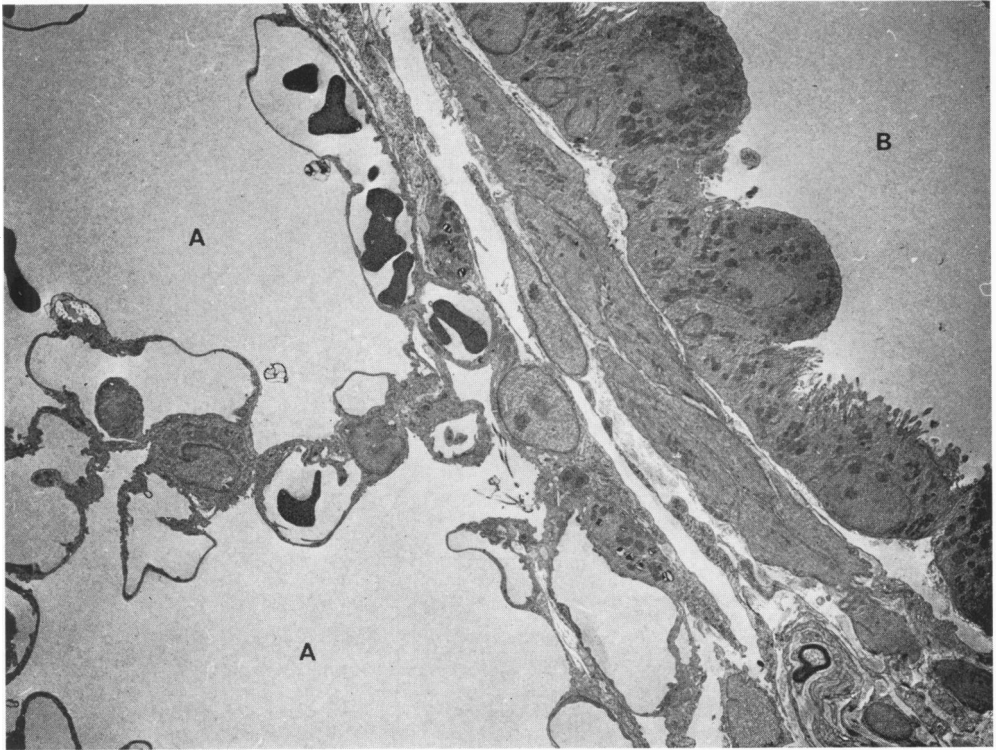
Key:

A = alveolus

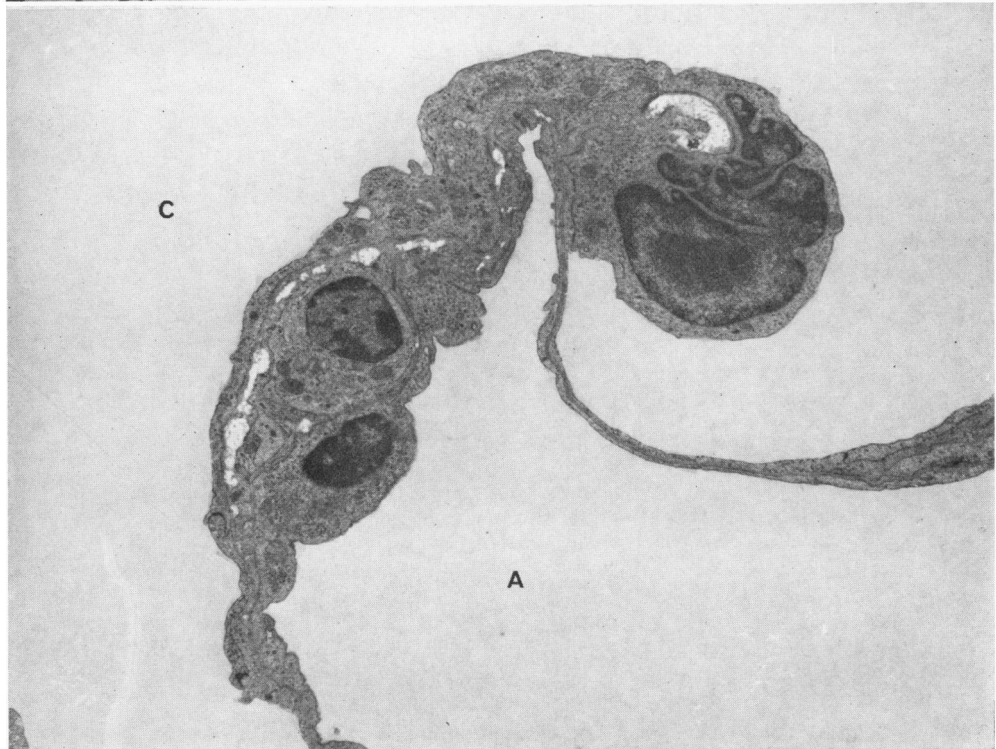
B = bronchiolar lumen

C = capillary lumen

- FIG. 1. A survey micrograph of the normal mouse lung, showing a small bronchiole and peripheral lung parenchyma. \times 2,000.
- FIG. 2. The blood-air pathway in the normal mouse lung. The section shows the nucleus of an epithelial cell lining the alveolus, and the nucleus of an endothelial cell lining the capillary. \times 5,000.

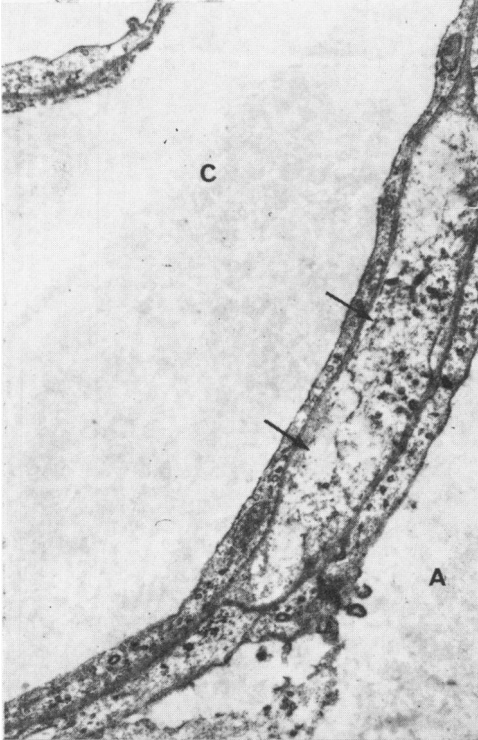
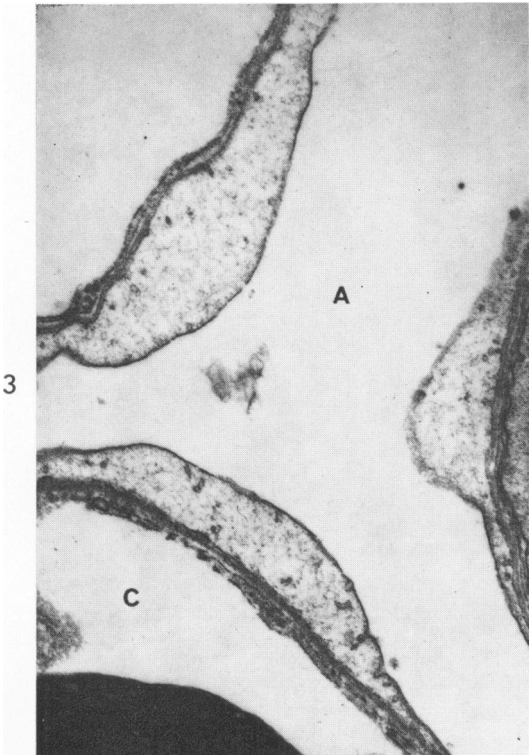


1

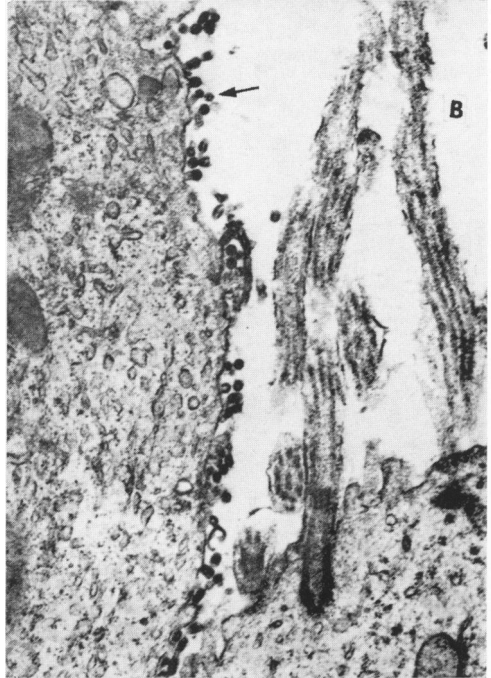
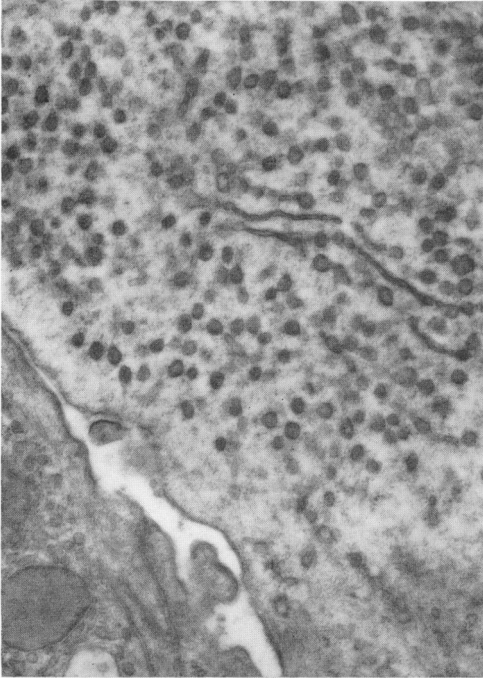
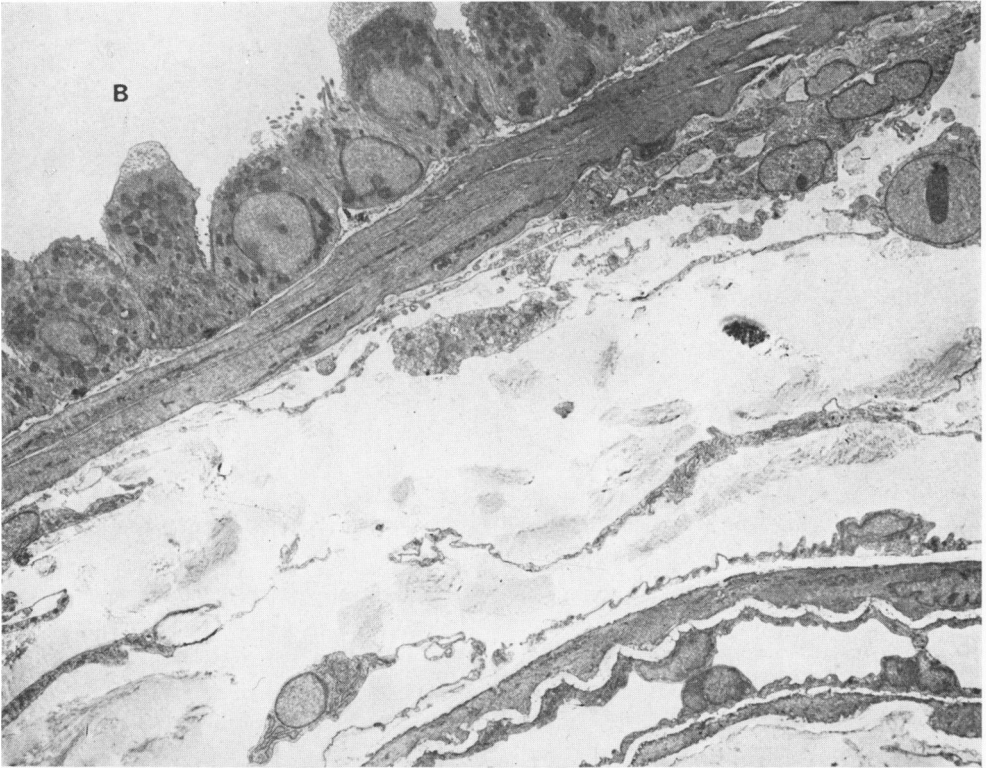


2

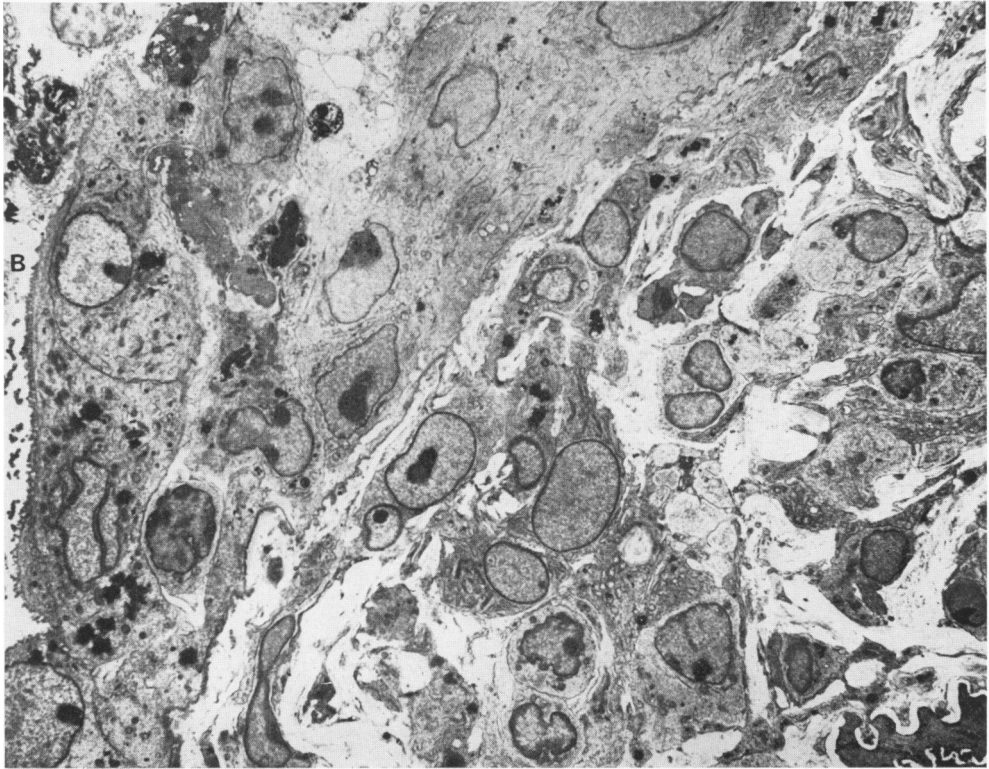
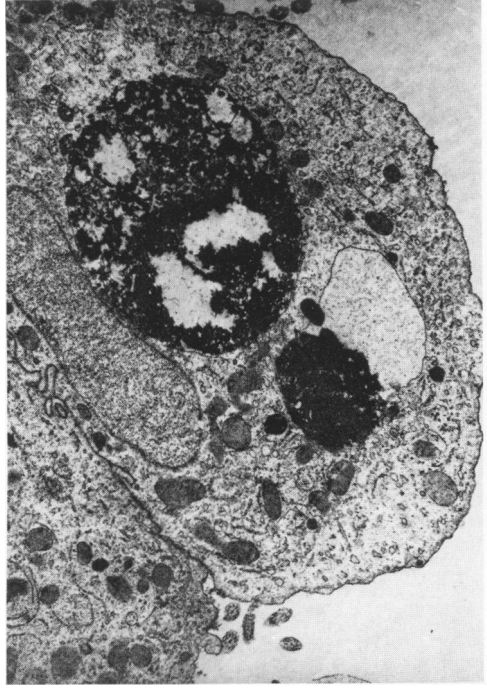
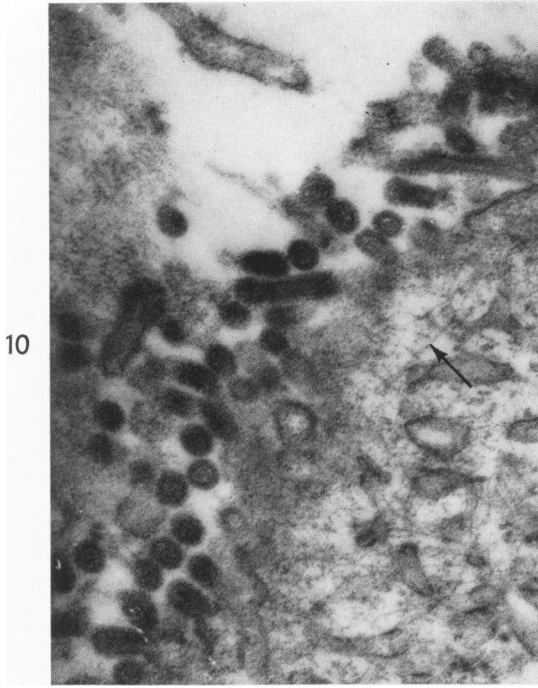
- Figures 3 to 6 are sections of infected mouse lung, 24 hours after inoculation.
- FIG. 3. Focal intracytoplasmic edema is seen in 3 alveolar lining cells. $\times 8,000$.
- FIG. 4. Marked intracellular edema in an alveolar lining cell is associated with rupture of the limiting membrane. The rupture of the membrane may, in this case, represent an artifact. $\times 11,000$.
- FIG. 5. Focal edematous areas in the capillary endothelium. Cross sections of 3 capillaries are seen here, each showing endothelial lesions, and each containing a red cell. The arrow indicates an area with increased pinocytotic vesicles in adjacent epithelial and endothelial cells. $\times 6,000$.
- FIG. 6. A region of basement membrane swelling and distortion. $\times 8,000$.



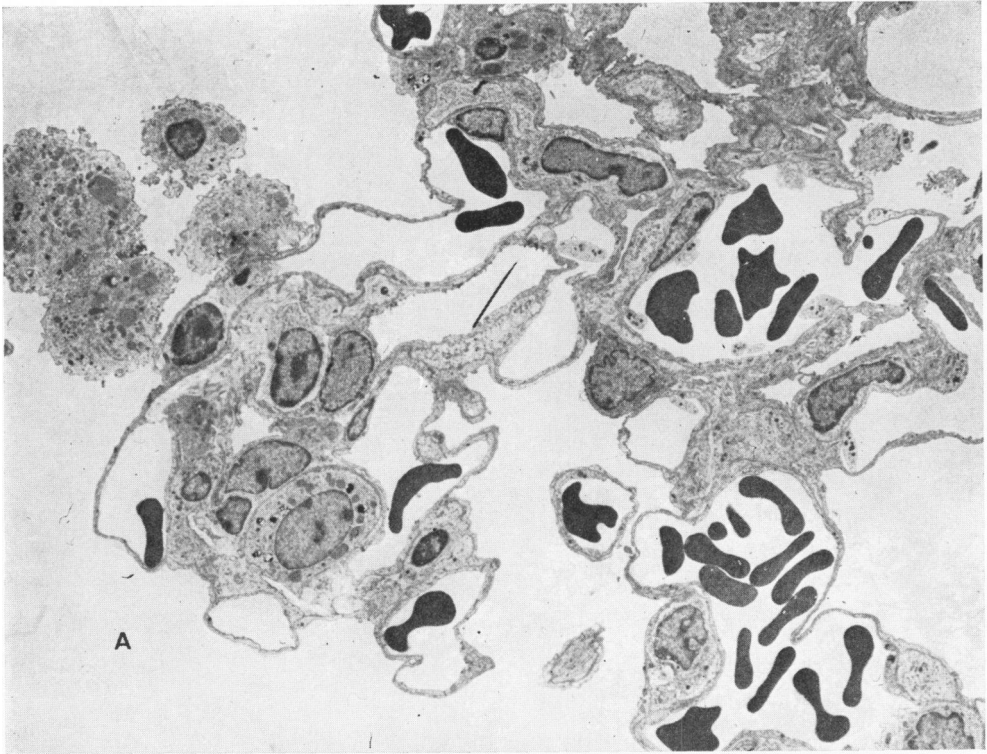
- FIG. 7. Section of an infected lung, 3 days after inoculation. Shown are a small bronchiole and its accompanying arteriole. The apical cytoplasm of the non-ciliated bronchiolar cells is edematous and protrudes into the bronchiolar lumen. The interstitial tissue between the bronchiole and the arteriole contains few cellular elements. $\times 2,000$.
- FIG. 8. Apical region of a nonciliated bronchiolar cell, 3 days after infection. The cytoplasm contains numerous small vesicles of endoplasmic reticulum; some appear to be arising from small tubular components. $\times 12,000$.
- FIG. 9. The virus is seen along the surface of a nonciliated bronchiolar epithelial cell (arrow). Viral production was never observed at the surface of the ciliated cells. $\times 10,000$.



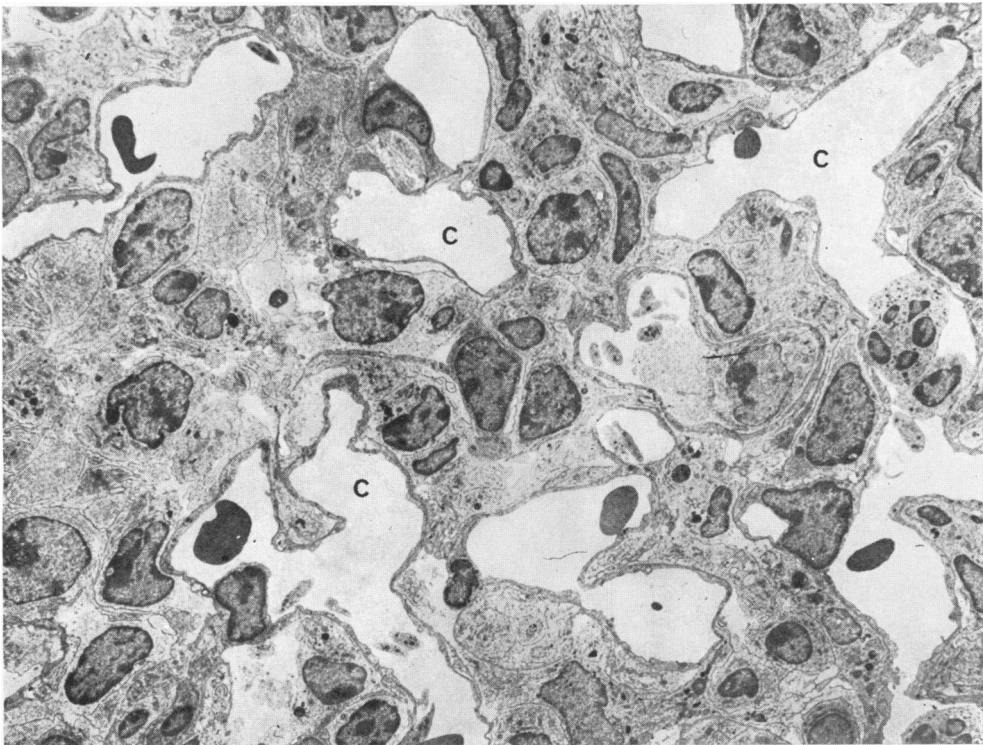
- FIG. 10. Viral particles maturing at the cell surface. The cytoplasm of the cell contains filamentous strands (arrow) which perhaps are viral ribonucleoprotein. $\times 40,000$.
- FIG. 11. A large, granular, osmiophilic inclusion is apparently compressing and displacing the nucleus of a bronchiolar lining cell. A smaller inclusion is present towards the surface of the cell. $\times 7,000$.
- FIG. 12. Section taken through a bronchiole and its accompanying arteriole (right lower corner) 7 days after inoculation. The bronchiolar epithelium is stratified, with many degenerative changes in the cells. Many of the surface cells have become necrotic and sloughed into the lumen. The interstitial tissue between the bronchiole and the arteriole is now completely infiltrated by cells, mostly of the mononuclear type. (Compare with Figure 7.) $\times 2,000$.



- FIG. 13. Peripheral lung parenchyma 4 days after inoculation. The capillaries are dilated and congested. A few mononuclear cells, perhaps desquamated alveolar epithelial cells or macrophages, are found free in the alveolar air spaces. $\times 2,500$.
- FIG. 14. At 1 week after infection, the alveoli are completely consolidated with mononuclear cells, with no remaining air space. $\times 2,000$.



13



14